Venice lagoon chlorophyll-a evaluation under climate change conditions: A hybrid water quality machine learning and biogeochemical-based framework

F. Zennaro [a,b], E. Furlan [a,b], D. Canu [c], L. Aveytua Alcazar [c], G. Rosati [c], C. Solidoro [c], S. Aslan [a], A. Critto [a,b,*]

[a] Department of Environmental Sciences, Informatics and Statistics, Ca' Foscari University of Venice, Venice, Italy
[b] Risk Assessment and Adaptation Strategies Division, Fondazione Centro Euro-Mediterraneo sui Cambiamenti Climatici (CMCC), Venice, Italy
[c] National Institute of Oceanography and Experimental Geophysics (OGS), 34010 Trieste, Italy

ARTICLE INFO

ABSTRACT

Climate change presents a significant challenge to lagoon ecosystems, which are highly valued coastal environments known for their provision of unique ecosystem services. As important as fragile, lagoons are vulnerable to both natural processes and anthropogenic activities, and this vulnerability is exacerbated by the impacts of climate change, which are likely to result in severe ecological consequences. The complexity of water quality (WQ) processes, characterized by compounding and interconnected pressures, highlights the importance of adequate sophisticated methods to estimate future ecological impacts on lagoon environments. In this setting, a hybrid framework is introduced where Machine Learning (ML) and biogeochemical (BGC) models are integrated in a sequential modelling approach. This integration exploits the unique strengths offered by both models. The ML model allows capturing and learning linear and nonlinear correlations from historical data; the BGC interprets and simulates complex environmental systems subject to compounded pressures, building on identified causal relationships. Multi-Layer Perceptron (MLP) and Random Forest (RF) ML algorithms are trained, validated and tested within the Venice lagoon case study to assimilate historical WQ data (i.e., water temperature, salinity, and dissolved oxygen) and spatio-temporal information (i.e., monitoring station location and month), and to predict changes in chlorophyll-a (Chl-a) conditions. Then, projections from the BGC model SHYFEM-BFM for 2019, 2050, and 2100 timeframes under RCP 8.5 are integrated into the ML model (composing the hybrid ML-BGC model) to evaluate Chl-a variations under future biogeochemical conditions forced by climate change projections. Moreover, the SHYFEM-BFM standalone Chl-a projections are also used to compare the hybrid and the BGC scenarios. Annual and seasonal Chl-a predictions are developed by classes based on two classification modes (median and quartiles) established on the descriptive statistics computed on historical data. Results from the case study showed as the RF successfully classifies Chl-a with an overall model accuracy of about 80% for the median and 61% for the quartiles modes. Concerning future climate change scenarios, results revealed a decreasing trend for the lowest Chl-a values (below the first quartile, i.e. 0.85 μg/l) moving to the far future (2100), with an opposite rising trend for the highest Chl-a values (above the fourth quartile, i.e. 2.78 μg/l). On the seasonal level, summer remains the season with the highest Chl-a values in all scenarios, although in 2100 a strong increase in higher Chl-a values is also expected during the springtime one. The proposed hybrid framework represents a valuable approach to strengthen both multivariate Chl-a modelling and scenarios analysis, by placing artificial intelligence-based models alongside biogeochemical models.

1. Introduction

Lagoons are highly productive ecosystems that provide a range of natural services valuable for society (Newton et al., 2018; Anthony et al., 2009). They are characterized by a high rate of dynamic changes in the natural environment and significant biological productivity and

---

diversity that sustain the socio-economic development of coastal communities. However anthropogenic activities can lead to the degradation of natural resources, posing the need for environmental monitoring and regulation (Lloret et al., 2008; Solidoro et al., 2010). As transition systems between land and sea, and due to their restricted exchange with the adjacent sea, coastal lagoons are particularly prone to eutrophication (i. e., the phenomenon of excessive algal productivity, due to over-stimulation of plant growth and disruption in the production and metabolism of organic matter (Cloern, 2001). A phenomenon that is also emphasized by the increasing population densities and/or the use of fertilizers for agriculture in the surrounding watershed (Anthony et al., 2009; Lloret et al., 2008). The Venice Lagoon ecosystem is extremely vulnerable to eutrophication, also considering the particular vulnerability of this area to climate change (Bednar-Friedl et al., 2022). Changes in climate conditions, i.e. variations in temperature and precipitation patterns, are expected to affect WQ by: *i)* changing in timing and delivery of river input and associated nutrient load (Salon et al., 2008), with cascading impact on biogeochemical dynamics (Cossarini et al., 2008) and related ecosystems' goods and services (Canu et al., 2010), and *ii)* overheating water under extreme heat waves, triggering the migration (or death) of individual organisms (Caretta et al., 2022; Sen Gupta et al., 2020). Additionally, the continuous increase in human-made inputs applied to most agro-ecosystems has increased yields but may be offset by reductions in the quality of the natural capital (e.g., land degradation, pollution, depletion of natural resources) (de Backer et al., 2009); in turn, this may also contribute to WQ changes while altering nutrients river inflow inside the lagoon (Grafton et al., 2018). This range of interconnected pressures poses several research questions on future WQ status (Bednar-Friedl et al., 2022; Mack et al., 2019). The lagoon expected multiple pressures highlight the importance of adequate methods to estimate the future extent of climatic drivers and their ecological impacts on the fragile environment to support appropriate actions for climate change adaptation.

Recent advances in the field of Artificial Intelligence and deterministic modelling (such as biogeochemical, BGC models) have been massively applied to model, anticipate, and predict natural hazards, including harmful algal blooms, high turbidity, acidification, and anoxia in open ocean (Kwiatkowski et al., 2020), coastal areas (Uusitalo et al., 2022) and lagoons (Aslan et al., 2022; Chen et al., 2020; Morucci et al., 2020; Politikos et al., 2021). Deterministic models are based on only a set of well identified processes, assumed to be the most relevant for the considered aim, and cannot capture, nor describe, dynamics emerging from processes not specifically included in the model. Furthermore they rely on a-priori knowledge that is often extrapolated from controlled experiments, usually not fully representative of the real-world variability, and require mathematical description of natural processes that could be incomplete or inaccurate. Conversely, ML data driven approaches describe and reproduce observed pattern in data regardless the underpinning processes and can therefore capture relationships and dependencies that cannot be included and modelled by deterministic models. Nevertheless, often the adopted ML algorithms require a solid inductive knowledge, provided by the physics of the phenomenon at stake (or at least the understanding of it).

Conscious that ML needs a large volume of data covering proper range of variability to be trained, and shows high performing skills in a big data context (L'Heureux et al., 2017), the availability of high temporal resolute WQ monitored data within the Venice Lagoon has made it possible to develop a hybrid framework that combines ML and BGC models to unravel and model environmental systems even within the context of climate change scenarios. Therefore, a hybrid approach that take advantages of the growing availability of knowledge on processes, computational resources, and big volume of data has the potential to achieve more flexibility and full synergy among the strengths of deterministic BGC simulations and ML. The hybridization is intended in this study as a modelling approach involving the combination of deterministic-based numerical models and data-driven models as a part of the common modelling pipeline (Borisova et al., 2021). In this way, the hybrid modelling of biogeochemical marine and coastal processes benefits from both the interpretability of numerical simulations and the extrapolation and generalization capabilities of advanced ML methods. In particular, the hybridization involves incorporating the output, i.e., future projections, of the Venice Lagoon BGC model into a supervised ML algorithm, that is fine-tuned on a suite of WQ variables to predict Chl-a, that is a recognized eutrophication proxy (Vinçon-Leite & Casenave, 2019).

Building on this framework, this study aims at improving the understanding of Chl-a behaviour in the Venice Lagoon over the last ten years (2008–2019) and then evaluating the potential Chl-a variations under baseline and futures climate change conditions. To this end, a descriptive statistical analysis is preliminarily carried out to investigate the temporal variation of WQ variables, then a multivariate analysis with Random Forest (RF) ad Multi-Layer Perceptron (MLP) ML algorithms is performed. Future dynamics are investigated by integrating in the ML-model the projections of physical and biogeochemical state variables obtained with the SHYFEM-BFM BGC model (Melaku Canu et al., 2023) for the years 2019, 2050 and 2100. The focus is on the predictions of Chl-a future estimates under a climate change scenario that encloses all the expected changes and poses greater environmental stress, i.e., the business-as-usual RCP 8.5 scenario (Brazil et al., 2008; Intergovernmental Panel on Climate Change, 2014; Riahi et al., 2011).

In the next sections, after a brief description of the case study (Section 2), data, variables and methodological approach underpinning the joint ML and BGC modelling framework are explained (Section 3). Finally, results on future Chl-a scenarios from both the hybrid ML-BGC and the BGC standalone models are compared and discussed (Section 4).

2. Study Area

The Venice Lagoon (northern Adriatic Sea, Italy) is the largest lagoon system in Italy, with a total surface of approx. 550 km^2, and one of the largest in the Mediterranean Sea (Sfriso et al., 2009). It is a polymorphous shallow coastal environment with a mean depth of 1 ± 0.3 m and large canals connected with the sea through three inlets (i.e., Lido, Malamocco, and Chioggia) 10–15 m deep (Facca et al., 2014), characterized by the presence of a multiplicity of aquatic (e.g., salt marshes, shoals, and mud flats) and terrestrial (e.g., islands, coastal strips) habitats (Bernardi Aubry et al., 2021). The tidal seawater flowing through the three-port inlets amounts to approximately a third of the total volume of the lagoon at each tidal cycle (Gačić et al., 2004), with a hydrodynamic residence time of 1 to 3 days close to the inlets and 15–20 days to the mainland (Cucco & Umgiesser, 2006). Freshwater inputs arise from the regulated flow of 12 main tributaries from a drainage basin of about 1850 km^2, accounting for around 35 m^3 s^{-1} y^{-1}, with seasonal peaks in spring and autumn (Bernardi Aubry et al., 2021; Zuliani et al., 2005). Nowadays, the lagoon mostly is well-oxygenated (Çevirgen et al., 2020), and it might be classified as a well-mixed estuary (i.e., the water column is completely mixed, making the estuary vertically homogeneous), defined by a strong inshore salinity gradient (Bendoricchio & De Boni, 2005; Solidoro et al., 2004).

Due to its variability, the Venice case is analysed in this study considering the hydro-morphological characteristics of the lagoon, with a specific focus on its water bodies and related chemical and environmental features (case study in Fig. 1). Indeed, based on art.2 of the Water Framework Directive (WFD) (EC, 2000), and the Italian D.Lgs n.152/ 2006 on transitional waters, the lagoon is divided into 14 water bodies. These water bodies have been defined in relation to *i)* pressures affecting them, *ii)* the information available on the physicochemical and ecological status, and *iii)* their hydro-morphological features (ARPA Veneto, 2021). In the present study, data of 10 monitoring stations belonging to 7 water bodies; i.e., PC1 Dese, PC2 Millecampi Teneri, EC Palude Maggiore, ENC1 Centro Sud, PNC1 Marghera, ENC4 Sacca Sessola, CS Centro Storico in Fig. 1) are analysed.
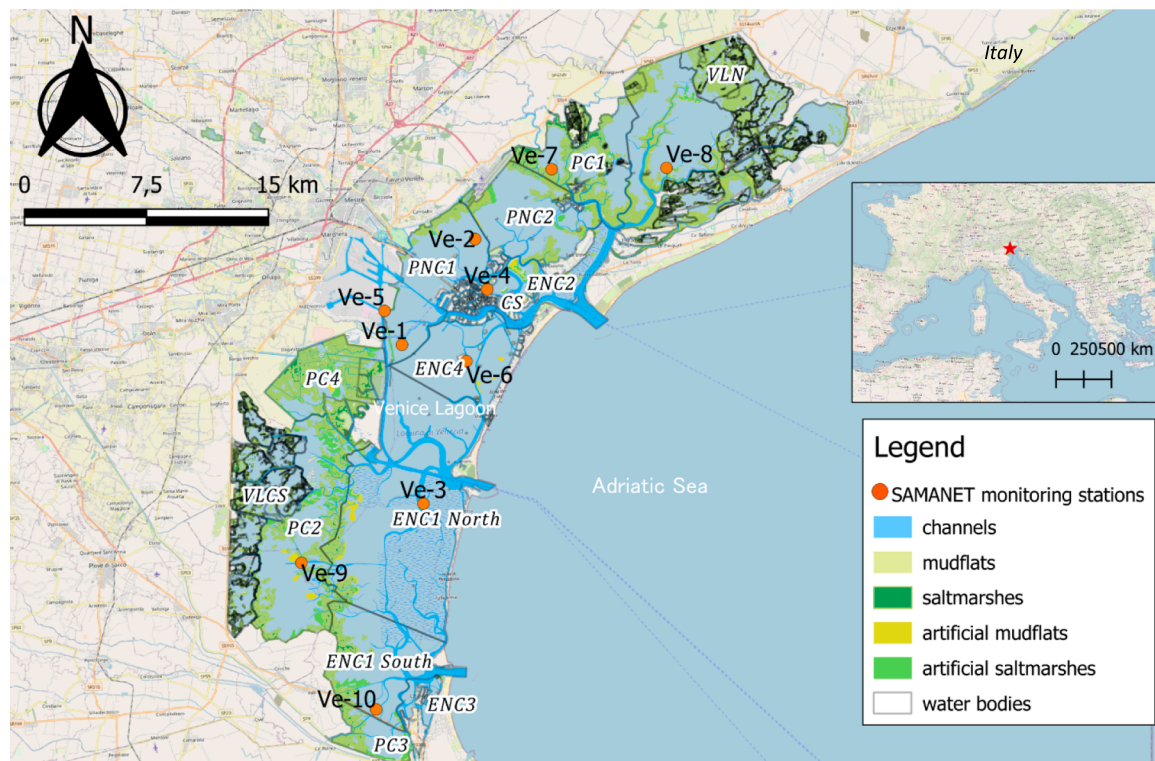
Fig. 1. Location of the Venice Lagoon and its hydro-morphological features. The 10 SAMANET sampling monitoring stations are marked by orange dots. (For interpretation of the references to colour in this figure legend, the reader is referred to the web version of this article.)

Considerable effort was undertaken in the past to reduce the pollution load into the lagoon (Runca et al., 1996). It has been estimated that a mean of 4000 tons of nitrogen and 180 tons of phosphorous per year are discharged in the lagoon environment from the drainage basin (MAV, 2008). During the last decades, the excess of nutrients in the water column has induced a series of algal blooms phenomena (Facca et al., 2014; Runca et al., 1996). In the 1970 s they were typically phytoplankton blooms (Chl-a up to 190 μg/l in 1978), then subsequently macroalgae, in particular nitrophilous opportunistic species, like *Ulva rigida*, which have become the dominant primary producers (in the shallow areas with high nutrient input and poor water exchange, *Ulva* outcompetes phytoplankton) (Facca et al., 2014; Solidoro et al., 2010).

Among the abundant algal blooms frequently observed and recorded during years (Facca et al., 2014; Sfriso et al., 1989, 2019), mentionable are the events of July 2013 and May 2017. During these events, an anomalous growth of *Ulva, Gracilaria, and Agardhiella* algae were observed as a consequence of particular meteorological cascading events featured by abundant precipitations (e.g., 800 mm for the period January-June 2013) and a subsequent heat wave (e.g., June 2013 maximum temperature between 28 °C and 30 °C) (ARPA Veneto, 2013). These events resulted particularly impactful due to brown discoloration of the water and fish mortality, which led to ecosystem services losses (e. g., reduction in food provisioning and habitat conservation).

3. Data and methods

A hybrid framework to evaluate past Chl-a behaviours and the possibility that the WQ equilibrium will be more likely to be altered by Chl-a variations under the mid and far future, is here proposed (Fig. 2). As mentioned earlier, this framework allows exploiting functionalities and strengths of two different types of models: a ML and a BGC model. In particular, the ML model is used to analyse historical data, then the hybridization of the ML model with the BGC model (herein hybrid ML-BGC model) is performed to compute baseline and future Chl-a

predictions under the RCP 8.5 scenario. Furthermore, the results of the ML-BGC model are compared with the projections obtained from the BGC model.

The following section presents the descriptive analysis of the data and variables used within this study (Section 3.1). Moreover, the hybrid ML-BGC framework is described, providing details on the design of the ML model (Section 3.2), as well as the scenario development (Section 3.3).

3.1. Data and variables analysis

The developed ML models are based on the WQ data acquired in the 10 monitoring stations of the Venice Lagoon SAMANET network[1] (see Fig. 1) for the 2008–2019 timeframe. Daily *water temperature*, *salinity*, and *dissolved oxygen (DO)* data are used as predictor variables in this study to estimate *Chl-a* levels. The limited availability of data on nutrients (e.g., nitrogen and phosphorous) concentration, showing very low temporal resolutions and coverage (i.e., seasonal observations from 2011 to 2019) did not allow to include these variables in the designed ML model, although they are undoubtedly relevant in driving Chl-a levels. Nevertheless, as a surrogate for this gap, nutrients are integrated in the framework as an additional input of the deterministic BGC model SHYFEM-BFM. The SHYFEM-BFM 3D coupled hydrodynamic and biogeochemical model applied to the Venice Lagoon (Melaku Canu et al., 2023), simulates the hydrodynamic, water temperature and

---

[1] The SAMANET Network consists of 10 automatic detection stations equipped with multi-parameter probes, presenting a fairly uniform distribution across the whole lagoon. These stations are designed to continuously acquire data on physical–chemical parameters (i.e., salinity, water temperature, pressure, dissolved oxygen, Chl-a, and turbidity) with a very high time–frequency (half-hourly services), allowing to capture seasonal variations in WQ and to study complex dynamics of interaction underpinning natural processes at a very short time scale (https://solve.corila.it/).
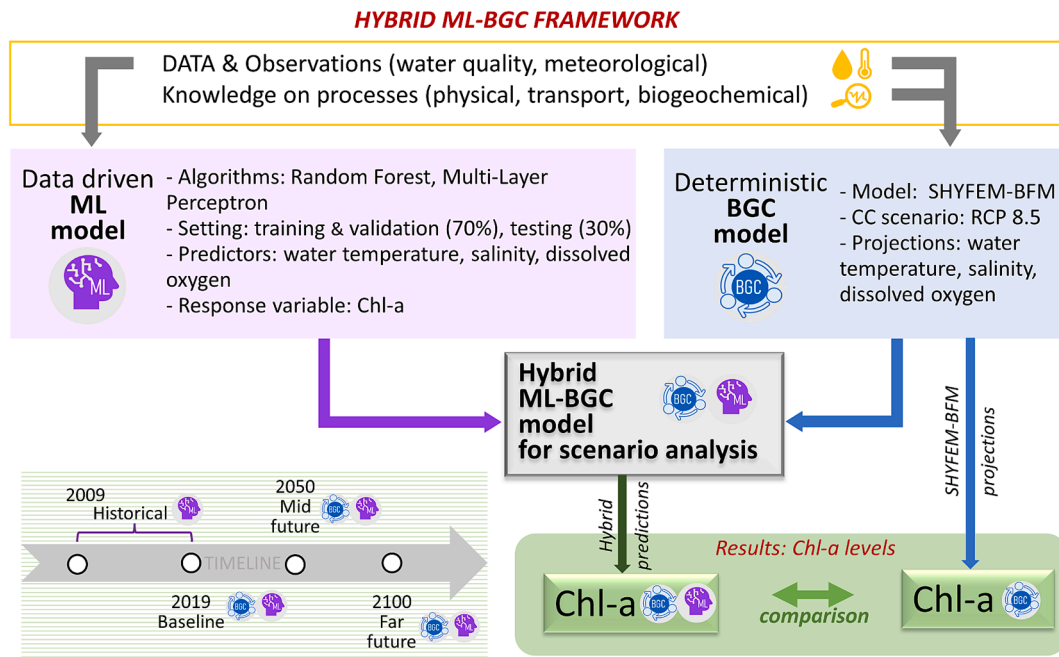
Fig. 2. Hybrid framework designed to outline Chl-a climate change scenarios.

salinity and the evolution in time of 54 biogeochemical state variables, on a staggered finite element grid consisting of 6017 nodes and 10,417 elements. The water column is discretized into 7 vertical layers.

In Table 1 the metadata of the datasets used within this study are resumed moreover, the descriptive statistics for the four datasets are reported in Table 2.

3.1.1. Historical data for ML model design

The dynamics governing the evolution of *Chl-a, temperature, DO,* and *salinity*, parameters indicative of the trophic state and used in lagoon classification, are multifaceted and interlinked (Ciavatta et al., 2008; Solidoro et al., 2010). The detail of variables' interrelations lays the ground for train, validate and test the reference ML model, which is built on the learning of variables' complex interdependences. As can be seen in the histograms in the Supplementary Material 1 (SM1), representing the values measured on the 10 monitoring stations, the WQ parameters and, in particular Chl-a, are not normally distributed. The Spearman rank correlation, which is a non-parametric test, is then considered the most appropriate to be applied to measure the degree of association among variables (in Figure SM2.a can be found the p-value test that confirms the no-random nature of presented correlations). The advantage of the Spearman rank correlation test is that it does not carry any assumptions on data distribution and is the appropriate correlation metric when variables are measured on a scale that is at least ordinal (Myers & Sirois, 2006). As far as the correlation matrix on historical data is concerned (Figure SM2.b), it can be seen that Chl-a is positively correlated with water temperature (0.46), possibly suggesting that temperature drives algae growth, while Chl-a is negatively correlated with salinity (-0.18), presumably linked to river discharge and related nutrient loads (Acri et al., 2020; Bendoricchio & De Boni, 2005; Solidoro et al., 2004). Analysing the Venice Lagoon WQ trends it is also noticed that lower salinity values generally correspond to higher nutrient and Chl-a concentrations. Moreover, several studies (Al-Taee, 2018; Håkanson & Eklund, 2010) indicated that salinity increase in aquatic ecosystems affects most plants and causes ionic and osmotic stresses and biochemical and morphological alterations, as well as a nutrient imbalance. In particular, Al-Taee, 2018 demonstrated that increases in salinity immediately reduce net carbon fixation rates, while affecting photosynthetic pigments, Chl-a, and carotenoids. Concerning DO and

Chl-a correlations, it is well known that DO is related to Chl-a, particularly during eutrophication events. When algal blooms eventually die, microbial decomposition severely depletes DO, creating a hypoxic or anoxic dead zone, lacking sufficient oxygen to support most organisms (Facca et al., 2014). Dead zones are found in many water bodies especially during summer (Politikos et al., 2021). Accordingly, in the matrix the Chl-a is negatively correlated (-0.34) with DO, following the influences of microbial oxygen consumption during degradation of organic matter of algal and vegetal origin (Acri et al., 2020; Baxter, 2019).

3.1.2. BGC projections from the coupled biogeochemical model

The development of Chl-a scenarios under future climate change conditions is based on projections from the Coupled biogeochemical model SHYFEM-BFM under both mid (2050) and far futures (2100) relative to the baseline (2019). The BGC model SHYFEM-BFM has been recently developed and applied to the Venice Lagoon (Melaku Canu et al., 2023), compared with field data, and used to perform simulations under climate scenarios (Melaku Canu at al., 2023).

The coupled model is based on SHYFEM (Umgiesser et al., 2004) an open-source hydrodynamic model, and on BFM (Vichi et al., 2020), an open-source biogeochemical model. SHYFEM solves the shallow water equations reproducing water levels and transports, heat transport and water temperature at each time step. The model computes on time the physical processes, the transport, dispersion, and transformation of biogeochemical variables according to the physical processes. A daily output of the state variables is provided. The Biogeochemical Flux Model (BFM) (Vichi et al., 2020) reproduces the state and dynamics of 53 state variables representing the carbon cycling, nitrogen, phosphorus, oxygen, and silica among water, non-living and living organic matter, taking into account microbial and plankton activity. The dynamics of the system depend on the state of the environment, represented by various external parameters e.g., solar radiation and water temperature, and evolve over time, influenced by changes in the physical state of the system. The model considers nine classes of plankton based on given functional characteristics, and divides them into three basic classes: primary producers (phytoplankton), predators (micro- and *meso-*zooplankton), and decomposers (bacteria).

The SHYFEM-BFM model is implemented using a mesh of over

Table 1
Dataset used for ML-models development and climate change scenario analysis.

	Dataset	Source	Timescale	Variables	Spatial resolution	Timeframe	Temporal resolution	Count for variable
ML model design	1	SAMANET network	Historical	water temperature (°C), salinity (PSU), dissolved oxygen (mmol/m³), Chl-a (µg/l)	10 stations: Ve1, Ve2, Ve3, Ve4, Ve5, Ve6, Ve7, Ve8, Ve9, Ve10	2008–2019	daily*	27,913
BGM projections	2	SHYFEM-BFM	Baseline	water temperature (°C), salinity (PSU), dissolved oxygen (mmol/m³), Chl-a (µg/l)	10 stations: Ve1, Ve2, Ve3, Ve4, Ve5, Ve6, Ve7, Ve8, Ve9, Ve10	2019 2050 2100	daily	3360
	3		Future climate change scenarios					
	4							

*SAMANET daily data are calculated as the average of half-hourly SAMANET net collected data.

10,000 elements and 6000 nodes. The model takes into account time variable inputs, boundary conditions and meteorological forcing such as river inputs of water and nutrients, exchange of water and biogeo-chemical variables with the sea, and meteorological forcing. Model inputs forcing and boundary conditions are set using observations and model projections. More specifically, meteorological forcing (including pressure, wind speed (u and v), total precipitation, relative humidity, mean air temperature at 2 m, solar radiation at the Earth's surface, thermal radiation at the ground) is determined using data generated by the CCLM model (COSMO CLM) for the RCP 8.5 scenario (Bucchignani et al., 2016). Data for ocean boundaries (water temperature, salinity, and biogeochemistry at inlets) are taken from the CMCC NEMO model (Reale et al., 2022; Solidoro et al., 2022). A bias correction is applied to the data set using real observations from 2019. The load from rivers is changed in its seasonal pattern in the scenario by modulating the river discharge according to the precipitation pattern in the basin, while the baseline nutrient concentration (2019) was maintained in accordance with ARPAV observations. Finally, sea level data are calculated by applying a trend with linear sea level rise between 2019 and 2100, with a rise of 0.71 m (Zanchettin et al., 2021).

3.1.3. Historical data and BGC projections: A comparison

This paragraph presents a preliminary comparative analysis of the historical and future (BGC projections) datasets to capture similarities and differences in trends and extreme values of the selected WQ variables. In particular, as a first exploratory data analysis, the descriptive statistics and the boxplots of the four datasets (as reported in Table 1 and Table 2) are presented in Fig. 3, evidencing important patterns on the historical (2008–2019), SHYFEM-BFM baseline (2019), mid (2050) and far (2100) future scenarios. In particular, looking at Fig. 3.a, in which Chl-a series are compared, the boxplots are relatively narrow, suggesting a low range of variability in Chl-a values across all the four time series. Moreover, Chl-a distributions appear right-skewed, indicating a non-normal distribution. The main difference emerges among extreme values, which are shown as outliers in the boxplot. In the Chl-a historical data, extreme values are more abundant than in the SHYFEM-BFM data and their magnitude (up to a maximum of 60.9 µg/l Chl-a) is much higher than the maximum of SHYFEM-BFM data (13.27 µg/l). While this could suggest a limited ability of the biogeochemical model SHYFEM-BFM to capture the full range of natural variability, it should be considered that the historical data incorporate the interannual variability from multiple years (2008–2019), while annual cycles are simulated with the SHYFEM-BFM model. This limited capability to capture the extremes is entirely to be expected, since the model does not represent all components of the system, but only a subset of them assumed to be relevant for capturing the main system features, and is therefore by design ineffective to reproduce all fluctuations and extremes. Furthermore, the model capability to reproduce extreme events is reduced by the lack of extreme variability in the external forcings (i.e., rivers input), which is filtered off by the (low) frequency of the forcing monitoring systems.

Comparing temperature boxplots (Fig. 3.b) it can be noted that medians of historical and SHYFEM-BFM for the year 2019 have coherent values (between 15.8 °C and 16.6 °C), which are expected to increase in the future, with values around 19.6 °C and 22.3 °C for the year 2050 and 2100 respectively. The interquartile range is wider in the historical data (-1.6 °C to 32.0 °C), and narrower in the SHYFEM-BFM outputs (2019: 2.4 – 32.9 °C, 2050: 4.1 – 8.2 °C, 2100: 34.0 – 39.0 °C). Comparing the interquartile ranges, to examine how the data is dispersed between each sample, it can be noted that lengths are similar, and outliers are not present. In the latter, the maximum water temperature values are reached in the 2100 dataset with 39.0 °C of daily mean. In general, the historical, 2050, and 2100 temperature-related series show a normal distribution instead the year 2019 seems slightly positively skewed.

As far as DO is concerned, box plots in Fig. 3.c show more dispersed data in the historical series and less ones in the SHYFEM-BFM
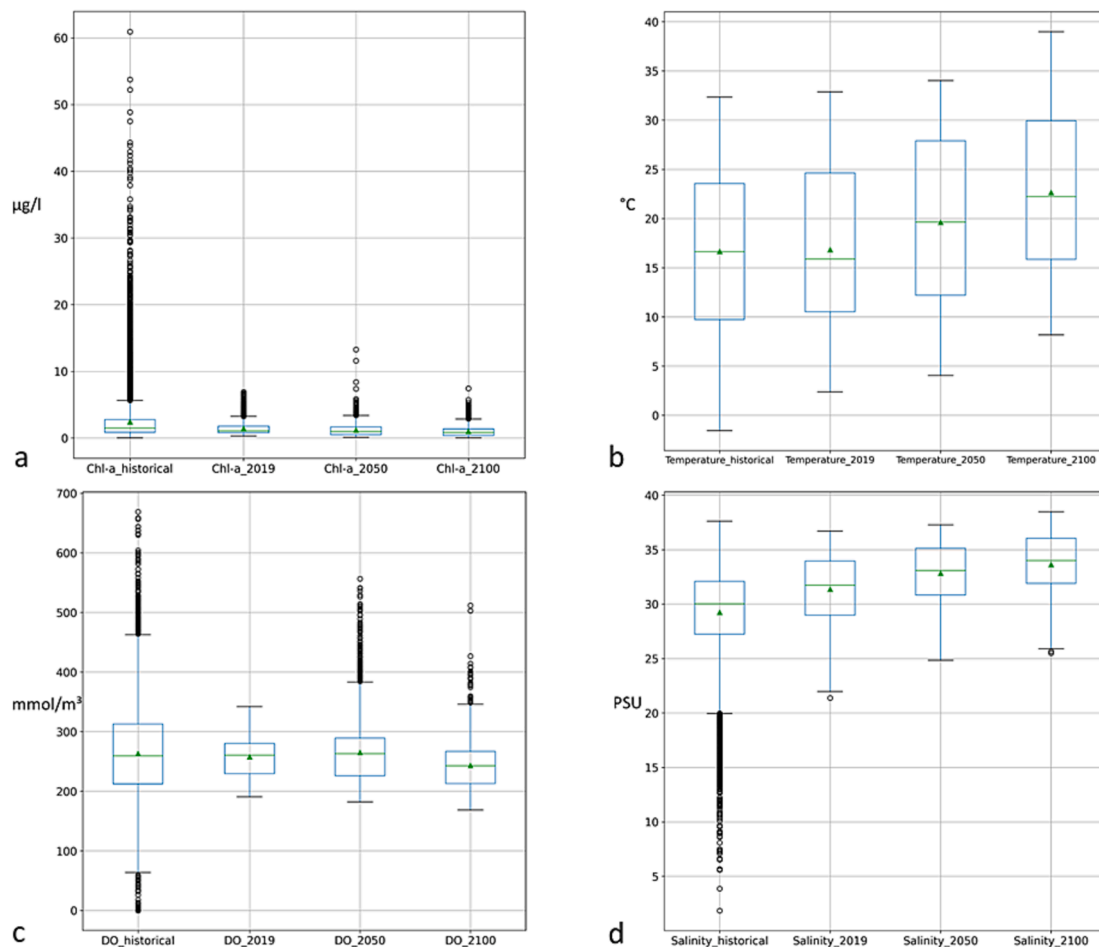
Table 2

Descriptive statistics for the four datasets: the historical period (2008–2019) measured by the SAMANET network, and the SHYFEM-BFM outputs for the baseline (2019) and future scenarios (2050 and 2100).

Historical (SAMANET) 2008–2019					SHYFEM-BFM 2019				
	Temperature (°C)	Salinity (PSU)	DO (mmol/m³)	Chl-a (µg/l)		Temperature (°C)	Salinity (PSU)	DO (mmol/m³)	Chl-a (µg/l)
mean	16.66	29.25	263.55	2.42	mean	16.84	31.38	258.02	1.41
std	7.72	3.96	71.73	2.97	std	7.79	3.10	32.14	0.91
min	−1.55	1.85	0.00	0.02	min	2.38	21.38	190.86	0.30
0.25	9.74	27.24	212.51	0.85	0.25	10.53	28.99	229.68	0.81
0.50	16.63	30.04	259.49	1.46	0.50	15.88	31.72	260.44	1.07
0.75	23.56	32.08	313.05	2.78	0.75	24.65	33.95	280.44	1.79
max	32.34	37.62	668.89	60.93	max	32.88	36.71	342.01	6.93
SHYFEM-BFM 2050					SHYFEM-BFM 2100				
	Temperature (°C)	Salinity (PSU)	DO (mmol/m³)	Chl-a (µg/l)		Temperature (°C)	Salinity (PSU)	DO (mmol/m³)	Chl-a (µg/l)
mean	19.62	32.85	265.20	1.20	mean	22.66	33.64	243.37	1.00
std	7.97	2.64	49.86	0.92	std	7.95	2.92	38.86	0.81
min	4.06	24.86	182.33	0.09	min	8.20	25.49	168.71	0.05
0.25	12.20	30.83	226.23	0.50	0.25	15.86	31.91	212.96	0.37
0.50	19.63	33.09	263.02	1.01	0.50	22.25	34.01	243.03	0.82
0.75	27.89	35.12	289.23	1.66	0.75	29.95	36.04	266.90	1.37
max	34.01	37.27	556.48	13.27	max	38.98	38.47	511.97	7.43

Fig. 3. Boxplots for Chl-a (a), water temperature (b), dissolved oxygen (c), and salinity (d) under the historical period (2008–2019, as measured by the SAMANET network), and the SHYFEM-BFM outputs for baseline (2019) and future projections (2049 and 2099). Mean values are indicated by the green triangles. (For interpretation of the references to colour in this figure legend, the reader is referred to the web version of this article.)

projections. Looking at the minimum and maximum values, great differences can be noted. As far historical data is concerned, the minimum value of the outlier (0 mmol/m³) is significantly lower compared to the SHYFEM-BFM, where the minimum value is reached in 2100 (168.7 mmol/m³). Nevertheless, this difference is not so relevant when looking at the minimum of whisker, in which historical data present a value of

212.5 mmol/m³ whereas SHYFEM-BFM is 213 mmol/m³. Similar behaviour can be mentioned for maximum values: the maximum whisker for historical data is 313 mmol/m³, while 289.2 mmol/m³ for the year 2050. The mean and the median values of historical data are similar to those of the 2019 and 2050 datasets (i.e., between 258 and 265 mmol/m³), while for 2100 a decrease in DO is projected by the

SHYFEM-BFM model (mean and median around 243 mmol/m^3).

Salinity is the variable that more strongly differs between historical and modelled data. Comparing the boxplots medians (Fig. 3.d), the value of the historical data (30.0 PSU) is slightly lower than the median value obtained with the SHYFEM-BFM for 2019 (31.7 PSU). Historical series present more dispersed data (larger interquartile range) and wider ranges of values than the SHYFEM-BFM model outputs. For the future scenarios, a further increase of average salinity is predicted by the SHYFEM-BFM model. This is mainly due to the SHYFEM-BFM model boundary conditions (see Section 3.1.2), where future model projections are dependent on the sea-level scenarios. As sea level is expected to be higher in the mid- long- term, a greater inflow of seawater into the lagoon is assumed, causing the salinity concentration increase.

3.2. ML model design

ML models for the classification and prediction of different Chl-a classes are developed building on two different classification modes (see paragraph 3.2.1 for details). Models are trained on historical (SAMANET) data (i.e., training), and then used to assign Chl-a class labels to the testing set, where the values of the predictors are known (i. e., *water temperature, salinity, DO, station* and *month*), but those of the response class label are not (i.e., testing). ML models are trained and validated (with the K-fold Cross-Validation[2] technique) on 70% of the dataset and tested in the remaining 30% (the two datasets have been randomly split) (Figure SM3). This approach is repeated by applying two different supervised ML algorithms, i.e., RF and MLP (see paragraph 3.2.2). The results are then compared and the model with the best performances is selected for the climate change scenarios analysis (see paragraph 3.2.3).

3.2.1. Classification modes

Among the various task in which ML can be applied (e.g., regression, classification, clustering (Zennaro et al., 2021), in the present work, ML is used to classify Chl-a values, as response variable in the designed models. In ML, classification is the process of predicting the class of given data points. Classification predictive modelling means approximating a mapping function (*f*) from input variables (*X*) to discrete output variables (*y*) (Marzban, 2009). In the context of this research, two classification modes are developed based on the descriptive statistics computed on historical (SAMANET) data (see Table 2): *i)* median classification of Chl-a values under and over the median value (*Mode 1*), *ii)* quartiles classification based on Chl-a quartiles (*Mode 2*). More specifically, the Chl-a threshold for the median classification is 1.46 μg/l; instead for the quartiles classification, the first quartile (Q1) corresponds to 0.85 μg/l, the second quartile (Q2) matches with the median, and the third quartile (Q3) is equal to 2.78 μg/l. Table showing the classes and related ranges applied to two modes are reported in the SM4.

3.2.2. ML models description

A huge variety of ML algorithms for classification exist, and their performances depend on the application and nature of the available data set (Kotsiantis et al., 2006). Considering the complex spatio-temporal dynamics and interactions occurring in the Venice Lagoon, two algorithms belonging to two significant families are implemented. In particular, the RF algorithm, from the decision trees family, and the MLP, from the artificial neural network (ANN) group, are applied. RF

and MLP show fundamental differences, and their architecture have been selected among a set of other possible ML algorithms (e.g., SVM, DT, LR) because they represent a good match for pursuing the objectives of this study (Aslan et al., 2022; Barzegar et al., 2020). Indeed, many examples can be founded in the literature demonstrating RF and MLP's good performances in capturing WQ data relationships, while providing good prediction and forecasting results for WQ indicators (Derot et al., 2020).

RF is a suitable approach to study biological systems because it is highly data-adaptive, applicable to both large and small problems, and able to account for correlation as well as for the interactions among different features (Ishwaran, 2012). Furthermore, it is known that this algorithm has no prior assumptions, is not too sensitive to missing data, and is adapted to manage nonlinear processes (Derot et al., 2020). Recent studies applying RF obtained high performance for forecasting phytoplankton and cyanobacteria distribution (Derot et al., 2020; Maier & Keller, 2019; Nelson et al., 2018). Tong et al. (2019) applied RF to simulate seasonal algal growth, also in relation to different nutrient levels. In their paper, they demonstrated that RF can be used to characterize the relationships between Chl-a concentrations and various environmental drivers, assessing the potential decline in Chl-a concentration with scenarios of reduction in total nitrogen or total phosphorous and an increase in temperature (Tong et al., 2019).

RF is an ensemble model that combines the predictions of multiple classification trees (Maindonald, 2013). Its purpose is to address the instability of individual trees, which can be influenced by specific subsets of training data (Hastie et al., 2009). By merging multiple trees, RF creates a more reliable and generalized model compared to single classification trees. Each tree is trained using a random subset of features and/or observations. Final predictions are obtained by averaging the predictions of all the classification trees. The RF classifier offers several hyperparameters for optimization, such as the number of features used, maximum tree depth, number of estimators (i.e., number of trees), sample split[3] and sample leaf[4]. In the SM5 an extract of the RF tree developed in the frame of this study is presented.

On the other hand, also MLP has been widely applied in literature to support the analysis and modelling of natural processes underpinning WQ variations across a wide range of water bodies (e.g. coastal areas, lakes, and lagoons). Among these, Nazeer et al. (2017) attempted to evaluate the performance of MLP algorithm to estimate Chl-a and suspended solids concentrations; similarly, Melesse et al. (2008) created a hybrid MLP-BP (Back Propagation) model to predict the level of Chl-a based on the correlation of monthly nutrients (and other WQ-related data) to Chl-a level in different data scenarios. Their model results demonstrated MLP-BP good performances. Ahmed et al. (2019), evaluated the correlation among several WQ parameters using MLP; finally, García Nieto et al. (2019) studied the relationship between algal atypical proliferation indicators and several biological and physical–chemical parameters through a MLP-based model.

MLP is a feedforward ANN: one neuron's output is propagated to the other neuron's input located in the next layer (Chen et al., 2020). More specifically, MLPs are general-purpose, flexible, and nonlinear models that, given a set of data, can virtually approximate any function with any desired degree of accuracy (Sarle, 1994). Therefore, MLPs can be used, for instance, when the form of the relationship between independent and dependent variables is unknown. Focusing on their structure, MLP models, like all ANNs, are composed by many layers of computing elements (called neurons) connected via weights which are determined by training the system through a training dataset (Miall, 1992). In particular, the MLP architecture developed for the Venice case study shows 5 neurons (i.e., *water temperature, DO, salinity, station,* and *month*), an

---

[2] *k*-fold CV: the training set is split into *k* smaller sets. For each of the *k*'folds', a model is trained using k−1 of the folds as training data; the resulting model is validated on the remaining part of the data (i.e., it is used as a test set to compute a performance measure such as accuracy). The performance measure reported by *k*-fold cross-validation is then the average of the values computed in the loop (source: https://scikit-learn.org/stable/modules/cross_validation.html).

---

[3] Sample split: min number of data points placed in a node before the node is split.
[4] Samples leaf: the minimum number of data points allowed in a leaf node.

output layer (*Chl-a*), and 'm' neurons in the hidden layer. A MLP, therefore, acquires a set of inputs included in the input layer), calculates a weighted average of them using weights, and, finally, uses some activation functions (*f*) to generate an output layer (figure SM5.b).

3.2.3. ML model selection

RF and MLP models are trained with both classification *modes 1* and *2*, and the hyperparameters are tuned using training and validation sets (figure SM3). Results of the accuracy (eq. (1) and F1 Score metrics (eq. (4) are compared to evaluate differences in performance between designed models. In particular, accuracy and F1 Score computed on confusion matrices have been (and still are) among the most popular adopted metrics in classification tasks (Chicco & Jurman, 2020). Model accuracy returns the number of classifications the model correctly predicts divided by the total number of predictions made. Mathematically, model accuracy is expressed as follows:

$$Accuracy = \frac{TP + TN}{TP + FP + TN + FN} \tag{1}$$

Where TP stands for 'True Positives', FP for 'False Positives', TN for 'True Negatives' and FN for 'False negatives'.

Recall (also known as sensitivity) (eq. (2) highlights the number of members of a class that the classifier identified correctly, divided by the total number of members in that specific class. Mathematically, model recall is defined as follows:

$$Recall = \frac{TP}{TP + FN} \tag{2}$$

Model precision (eq. (3) is the ratio between the True Positives and all the Positives. Mathematically, it is defined as follows:

$$Precision = \frac{TP}{TP + FP} \tag{3}$$

F1 score (eq. (4) is the weighted average of Precision and Recall, providing a way to express both concerns with a single score. Therefore, this evaluation metric takes both false positives and false negatives into account. F1 is usually more useful than the accuracy, especially under an uneven class distribution. The greater the F1 Score, the better the performance of the model is. Mathematically, the F1 score is defined as follows:

$$F1Score = \frac{2*(Recall*Precision)}{(Recall + Precision)} \tag{4}$$

Model evaluation and selection are performed considering the F1 Score that are assessed for each class under both *mode 1* and *2*. However, instead of having multiple per-class F1 Scores, macro average and weighted average are performed. Specifically, the macro average is computed by taking the arithmetic mean (also known as unweighted mean) of all the per-class F1 Scores; instead, the weighted average is calculated by taking the mean of all per-class F1 Scores while considering each class's support. In the context of a balanced class distribution as in the present work, these two metrics are interchangeable.

The model that show the best accuracy on the test set is selected for the predictions of future scenarios.

Moreover, indices can be used to assess the relative importance of predictors and make model outcomes more interpretable. Within this methodology, the Gini index (Breiman and Ihaka, 1984) is used to assess the impact of individual features. It measures the strength of the relationship between a feature and the target classes. However, one of its notable limitations is its nature, meaning it evaluates each feature in isolation and does not account for potential interactions with other features. This can lead to misleading results, especially when assessing features with a strong correlation, as the Gini index may assign low scores to certain features that are only effective when used in combination with others. However, due to its low computational requirements, Gini index is frequently used for estimating feature quality

in high dimensional domains, where the number of features incurs less manageable computational complexity of the more powerful feature selection methods (Čehovin & Bosnić, 2010).

3.3. Hybrid ML-BGC model for scenario analysis

Once the ML model that get the best performances on the test sets is selected the hybrid ML-BGC model is performed. The procedure consist in the incorporation of the SHYFEM-BFM outputs of *water temperature, DO*, and *salinity* variables into the ML model. The results are the developing of the Chl-a hybrid predictions for the years 2050 and 2100 and for the baseline period 2019. Chl-a classification for the projections of SHYFEM-BFM standalone is also performed to compare them to the results from the hybrid ML-BGC model. Finally, an insight analysis of the hybrid model baseline and future predictions is developed for each season (winter, spring, summer, and autumn). The model estimates each day to which class Chl-a values will belong (i.e., under/over the median -*mode 1*, and in one of the four quartiles -*mode 2*). The results are organized into plots that can help in the visualization of present and future (baseline, mid, and far future) potential Chl-a shifts.

4. Results and discussion

4.1. ML model selection

As detailed in Section 3.1, the dataset used for the ML model design includes 27,913 observations (i.e., corresponding to the number of days monitored by the SAMANET stations) of 6 WQ-related variables (i.e., water temperature, salinity, DO, station, month, and Chl-a). Classification *mode 1* and *2* are computed, and the performances in the test set are evaluated and compared through accuracies ad F1 Scores (session 3.2.3). Table 3 reports results obtained from the two model types (RF and MLP) under the test set. Differences can be observed between the two algorithms, but generally RF's performances result higher under both modes. Indeed, for the median classification, RF shows a 0.80 accuracy and F1 Score; instead, the MLP has 0.73 and 0.75 accuracy and F1 Score respectively. Furthermore, for the quartiles classification, RF reports 0.61 for both the evaluation metrics, rather than the MLP with an accuracy of 0.50 and a F1 Score of 0.49. Within the median classification the MLP performs slightly better for the 2nd class (values over the median), compared to class 1 (values below the median), with F1-score equal to 0.75 instead of 0.72. Conversely, the RF shows the same result for the two classes (0.80). As far as the quartiles classes are concerned, it can be noted that both models perform better results for the first and fourth classes (F1 Scores around 0.7) but are less able to catch the second and the third ones (F1 Scores between 0.51 and 0.52).

Globally, the RF results more stable and perform better than MLP; accordingly, it is selected as the most suitable model and best candidate to compute future climate change scenario analysis. In Fig. 4 the confusion matrices of the *modes 1* and *2*, as well as the histograms comparing the test set values and the RF predictions are reported. In particular, the main diagonals of confusion matrices (Fig. 4.a and 4.b) show that for both classification modes, RF models are able to classify correctly the majority of values (high percentage and count of values are predicted in the correct class). Within the quartiles classification, the percentage of false classification decreases as moving further away from the main diagonal, indicating that the model rarely misclassifies more than one-distance class (e.g., only 1.1 % of the time, it assigns the '1st quartile' class to a '4th quartile' observed data).

The histograms, Fig. 4.c and 4.d, show that RF slightly overestimates predictions in the 'under the median' class, with cascading effect of a minimal underestimation of values 'over the median'. As far as the quartiles classification is concerned, it can be observed that the 1st quartile is the one most overestimated, followed by the 4th quartile, as they include extreme values, while the two central classes (2nd and 3rd quartiles) are predicted fewer times than in the true values.

Table 3
MLP and RF model performances for the two classification modes.

		Multi-Layer Perceptron (MLP)				Random Forest (RF)			
Mode 1:median classification	Test set Accuracy:	0.73				Test set Accuracy:	0.80		
	F1_score:	0.73				F1_score:	0.80		
		precision	recall	F1 Score			precision	recall	F1 Score
	class 1	0.75	0.69	0.72		class 1	0.80	0.81	0.80
	class 2	0.72	0.77	0.75		class 2	0.81	0.79	0.80
	macro avg	0.74	0.73	0.73		macro avg	0.80	0.80	0.80
	weighted avg	0.74	0.73	0.73		weighted avg	0.80	0.80	0.80
Mode 2: quartiles classification	Test set accuracy:	0.50				Test set accuracy:	0.61		
	F1_score:	0.49				F1_score:	0.61		
		precision	recall	F1 Score			precision	recall	F1 Score
	class 1	0.56	0.65	0.60		class 1	0.71	0.74	0.72
	class 2	0.46	0.35	0.40		class 2	0.54	0.50	0.52
	class 3	0.44	0.36	0.40		class 3	0.51	0.51	0.51
	class 4	0.49	0.62	0.55		class 4	0.69	0.69	0.69
	macro avg	0.49	0.50	0.49		macro avg	0.61	0.61	0.61
	weighted avg	0.49	0.50	0.49		weighted avg	0.61	0.61	0.61
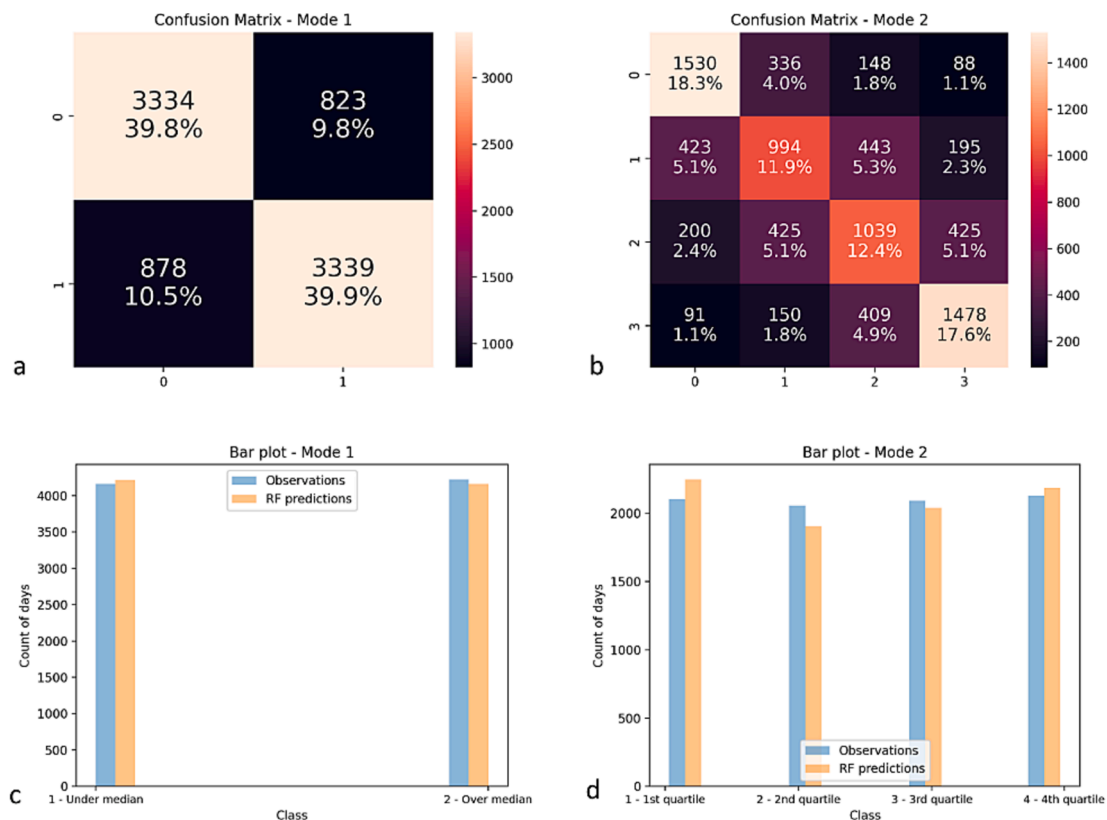
Fig. 4. RF performances. Confusion matrices of the Mode 1 – median classification (a) and Mode 2 – quartiles classification (b). Histograms of the counts of the total amount of days per class under the classification Mode 1 – median classification (c) and Mode 2 – quartile classification (d), comparing the test set (observations) and the RF predictions.

The Gini index used to assess the relative importance of predictors and make model outcomes more interpretable, (Han et al., 2016) (Fig. 5) suggests that temperature is the most relevant input in the model with about 30% of relative importance, followed by salinity (24%). Then, DO, with approximately 23%, and information on month of WQ data acquisition and location of monitoring stations showing approximately the 13% and 11% of relative importance respectively, compared to the other model variables. It must be noted that stations and months' relative importance have to be weighed, also considering the Gini index's

tendency to give more importance to the features with high cardinality; therefore, variables with few cardinal numbers, like the latter, can result in less significance for the model.

4.2. Scenario analysis

The hybrid ML-BGC model, obtained by combining the RF and the deterministic SHYFEM-BFM model, is applied to estimate both annual and seasonal Chl-a changes across the 10 Venice Lagoon stations for the
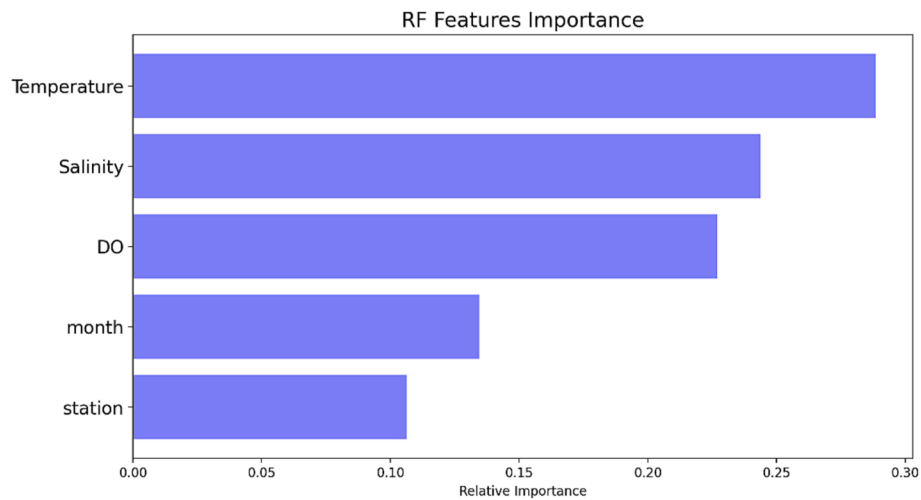
Fig. 5. RF model feature importance calculated with the Gini index.

years 2019 (as baseline), and 2050, 2100 (as mid and far future), under the RCP 8.5 climate change scenario. The results from the hybrid model are compared with the projections performed by the SHYFEM-BFM model standalone.

4.2.1. Annual-based scenario analysis

Annual variations in Chl-a values are shown in Fig. 6 comparing SHYFEM-BFM Chl-a projections (full-colour bars) with hybrid ML-BGC model predictions (diagonal lines bars). In particular, the SHYFEM-
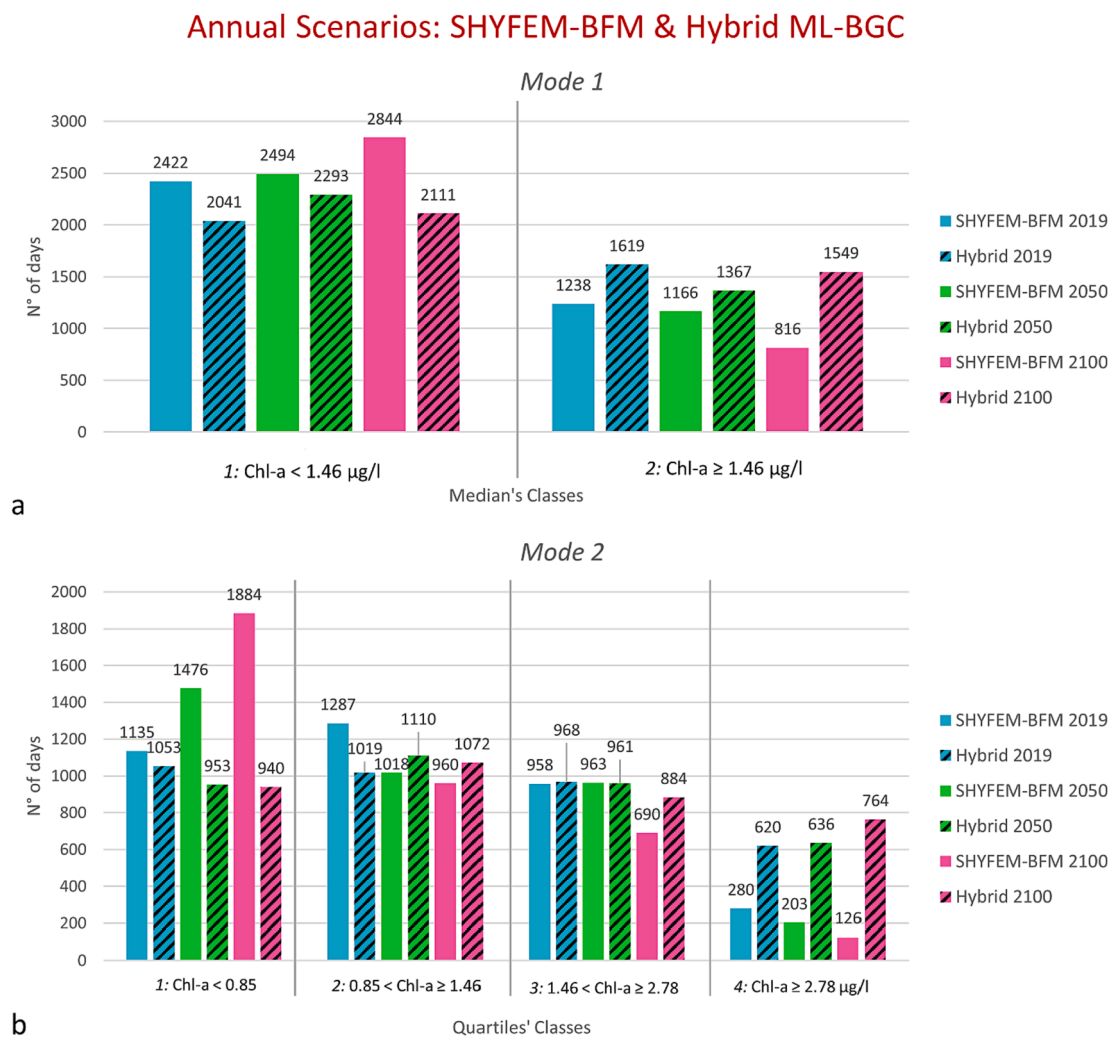

Fig. 6. Comparison among SHYFEM-BFM Chl-a projections (full colour) and hybrid ML-BGC predictions (diagonal lines) a) under the mode 1 – median classification; b) Mode 2 – quartiles classification. The height of the bars indicates the total number of days across the 10 stations considered in this study.

BFM projections, under the median classification (Fig. 6.a), evidence an increasing number of days when Chl-a assumes values below the median (class 1) moving from the mid to the far future. On the contrary, hybrid predictions indicate an increase in class 2 elements in the far future.

When looking at the model run under the *mode 2* (i.e., with quartiles classes, Fig. 6.b), in both the mid and far future, the SHYFEM-BFM Chl-a projections mainly fall within the 1st quartile; moreover, moving from 2050 to 2100, a significant increase in the number of days expected in this 'lower Chl-a's values' class can be seen. On contrary, in the other three classes, the total number days of Chl-a projections decrease from 2050 to 2100, until reaching less than 150 days per year for the 4th quartile in 2100. This decreasing trend in the BGC model projections depends on two main factors: *1)* The model design provides for a decrease in nutrient load from the watershed, which translates into decreased availability of nutrients in the lagoon system that is negligible in the mid future and relevant in the far one.*2)* Temperature increase leads to anticipation of phytoplankton blooms and variation in bloom phenology. Spring blooms are shorter and have lower Chl-a concentrations than in the baseline simulation.

Focusing on the comparison between SHYFEM-BFM and hybrid ML-BGC predictions, the 2nd and 3rd classes appear fairly similar across the various scenarios. On contrary, there is an inverse trend for the 1st and 4th classes. Overall, looking at the patterns of the hybrid model between the two extreme classes in the mid and far future, Chl-a values less than 0.85 µg/l (1st quartile) tends to decrease, while values greater than 2.78 µg/l (4th quartile) tends to increase. These changes could be related to the projected increasing temperatures in the future, which could lead the lagoon to an increment of periods in which the environmental conditions trigger an increased algae proliferation (and so, higher Chl-a values) and, as a consequence, the potential rising in eutrophication events.

These opposite trends between SHYFEM-BFM and the hybrid ML-BGC can be ascribed to the peculiarities of these two models: one (SHYFEM-BFM) based on causal relationship, the other (hybrid ML-BGC) based on correlation learning supported by the integration of past observations with predictions. Indeed, ML is better performing on detecting extreme values, compared to the SHYFEM-BFM. Moreover, discrepancies in values' trend can be attributed also to the differences among the input variables used by the two models (e.g. nutrients are included only into the BGC one; see Section 3.1). Furthermore, other differences may derive from the fact that the SHYFEM-BFM is a fairly complex biogeochemical model, but despite its relative complexity, it does not account for all processes that instead are captured by ML methods directly from data. By construction, even the most complex models obviously remain a simplification, and for this reason data assimilation is increasingly used in biogeochemical modelling (Teruzzi et al., 2019) to correct and improve the model's predictions. On the other hand, the numerical equations applied by BGC models are able to detect changes and shifts on the investigated systems that may not be captured by a ML method, even though during the investigated time-frame, such ecosystems' behaviours have not manifested. In this case indeed, the algorithm has not been able to learn that changes and shifts during the training phase, and therefore is not even capable to predict them.

Accordingly, combining a ML model with a BGC model undoubtedly offers advantages of integrating the causal approach with a method that learns directly from the data and, in case of Chl-a, enables to predict extreme values that the BGC model alone is not capable to reproduce. Further evidence of this pattern can be seen in the ML-BGC hybrid scenarios, where there is a long-term increase in Chl-a values classified in the highest classes. This finding aligns with the latest scientific research on climate change, which suggests that such changes are contributing to shifts in WQ parameters that can lead to harmful phenomena like eutrophication, hypoxia, and marine heat waves (Breitburg et al., 2018; Glibert, 2020; Jane et al., 2021; Lloret et al., 2008; Shalby et al., 2020).

4.2.2. Seasonal-based scenario in-depth study

Seasonal future variations in Chl-a values are here presented to deepen the infra-annual variability of the Venice lagoon system, which is the result of the overlay of the seasonal evolution of light and temperature, as well as of the non-cyclic development of dissolved nutrients loads, that are discharged into the lagoon by the tributaries and other point sources (Solidoro et al., 2004). Looking at the past, it is reported from the literature (Sfriso et al., 1992; Solidoro et al., 2010) that in the Venice Lagoon, Chl-a has shown a seasonal trend corresponding to the occurrence of a first moderate bloom in those areas presenting high nutrients concentration (i.e. near inland areas), around May (i.e., spring). Then, after a temporary regression, more massive blooms have been used to happen in July and August (i.e., summer).

Concerning the mid and far future, the hybrid ML-BGC model applied across the entire year show, in general, an estimation of Chl-a in the lower classes compared to the higher ones. However, if we look at the different seasons the model predictions reveal interesting findings. Fig. 7 reports the rose charts with the result of this analysis, showing the seasonal variations of the hybrid predictions respectively for the baseline scenario 2019, the mid future 2050, and the far future 2100, and against the classification modes *1* and *2*. Under the *mode 1* in Fig. 7.a, as expected, it can be seen that, in all three scenarios, in autumn and winter seasons, when the water temperature is lower and consequently oxygen solubility is higher, the majority of Chl-a values are predicted in the 'under the median' class (i.e., class 1); instead within the summer season, corresponding to higher temperatures, Chl-a is projected to be comprehensively 'over the median' value (i.e., class 2). The most relevant difference across the three scenarios is that moving from the 2019 to 2050 and then 2100 there is a strong increase in the 2nd Chl-a class during spring (from 3.9 % in 2050 to 13.9 % in 2100). In particular, until 2050 summer season is expected to be the one with more frequency of 'over median' Chl-a values (10.7 % in 2019 and 12.8 % in 2050), a pattern that is expected to change in the far future (i.e. 2100), in which also spring is likely to present high Chl-a values (13.9 %), reaching almost the same amount of 'over the median' days as classified in summer (14.9 %). This pattern indicates that in the far future, under business-as-usual conditions, also spring is foreseen to become more prone to higher Chl-a value and, eventually, to eutrophication events. This behaviour is also in agreement with the output of the SHYFEM-BFM model, where the increasing annual water temperature will result in a shift in the Chl-a production, that will be anticipated in spring due to the earlier optimal conditions for algal proliferation (e.g., temperature around 25 °C, abundant light, and stable wind conditions (Glibert, 2020); see also paragraph 3.1.3). Finally, also autumn seems to change slightly behaviour in 2100, as it is expected that the 2nd class will increase also in this season (from 4.5% in 2019 to 7.5%).

Looking at the hybrid predictions under the *mode 2* (Fig. 7.b), the same trends observed under *mode 1* can be noted: in winter and autumn prevalence of 1st and 2nd classes on one side, and in summer prevalence of 3rd and 4th classes on the other one. Focusing on the two extremes (1st and 4th quartile) it is worth pointing out that the presence of values in the first class decreases from 2050 to 2100 for all seasons except for winter. In particular, in spring and summer periods are reduced to about a dozen days (0.1%), highlighting that is not estimated (for the far future) to have Chl-a values under 0.85 µg/l during the warm semester. In all the scenarios we can see that higher values in Chl-a are projected to be mainly in summer (around 13% in all the scenarios), confirming that is expected to remain the season more prone to eutrophication events. As far as spring is concerned, aligned with the *mode 1*, an increasing number of days predicted in the higher values class (4th quartile) shifting towards the far future (from 1.9% in 2019 to 2.8% in 2050, and 6.8% in 2100) is estimated.

This estimated increasing pattern for the higher Chl-a classes, together with the expected increase in Chl-a levels during the spring season, not just in the summer, appears to be misaligned with the goals of the EU reference Mission, i.e. Starfish 2030 'Restore our Ocean and
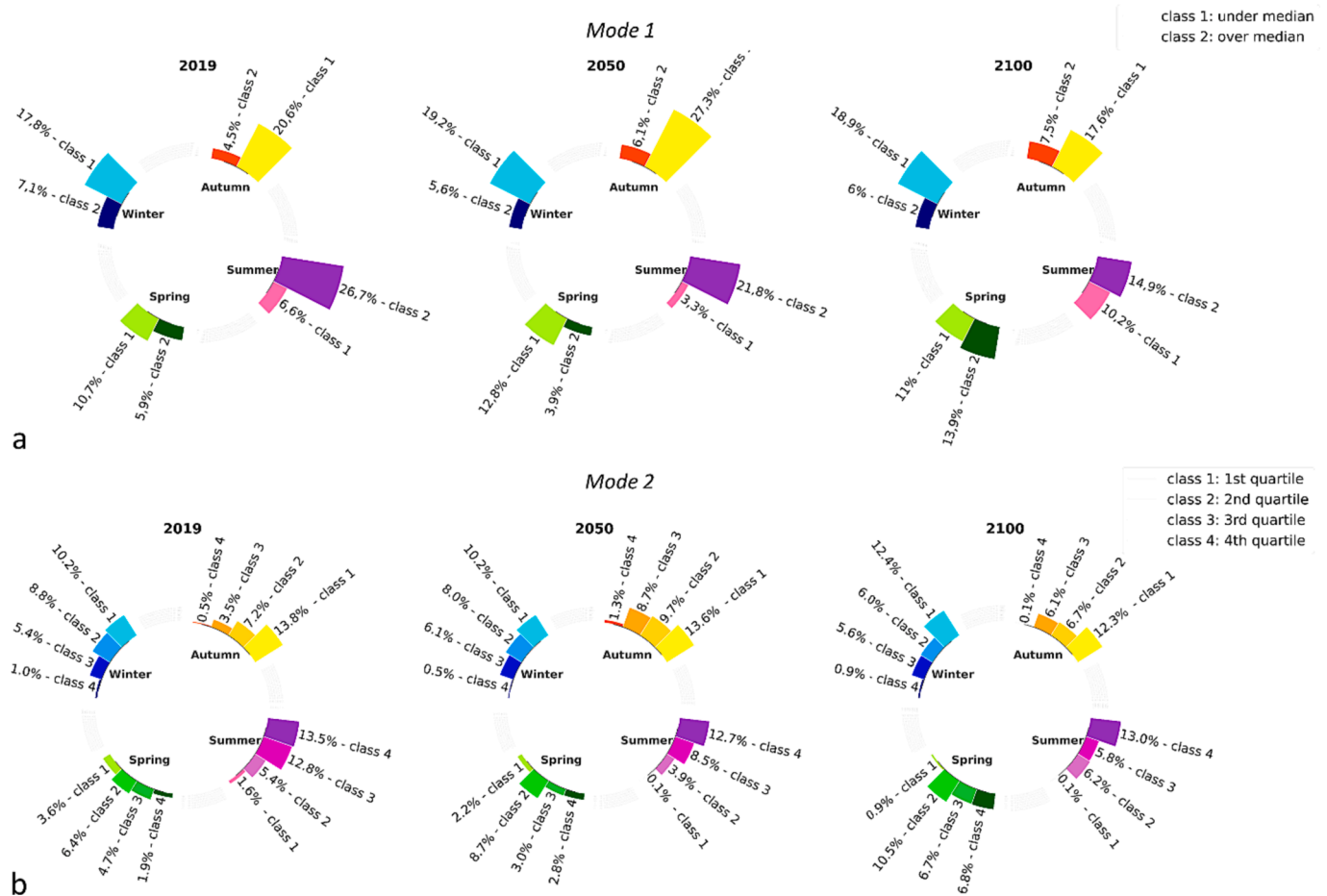
Fig. 7. Seasonal variations of hybrid ML-BGC predictions under a) the mode 1- binary classification, and b) the mode 2- quartiles classification, for the baseline scenario 2019, mid future 2050, and far future 2100.

Waters Report of the Mission Board – Healthy Oceans, Seas, Coastal and Inland Waters'. Specifically, these estimations paint a situation for the Venice Lagoon that deviates from one of the key objectives of Starfish 2030: to achieve zero pollution of our oceans and waters by 2030, which includes reducing nutrient pollution and eutrophication by at least 50%. At the same time, these results should be seen as a warning to raise public awareness and engagement on the future risks of eutrophication.

Furthermore, based on the latest advances in computer science and biogeochemical modeling, the results presented in this study contribute to strengthening the digitalization of monitoring, reporting and analysis processes. Thus aligning the existing methodologies with another key Mission 2030′s goal: digitalization in environmental assessment.

5. Conclusion

The present study describes a hybrid framework combining ML and BGC models to develop mid (2050) and long term (2100) Chl-a scenarios. The framework explores interrelations among three WQ (i.e., water temperature, DO, and salinity) and two spatio-temporal (i.e., location of monitoring stations and month of WQ data acquisition) variables to evaluate Chl-a. In particular, the Chl-a's future levels estimation is performed considering the 'business-as-usual' RCP8.5 scenario, as the pathway that poses the strongest environmental stresses, including intense meteorological and hydrological changes. The analysis is focused on the Venice Lagoon as one of the worldwide most relevant environmental and socio-economic systems and, at the same time, one of the most vulnerable and prone to be affected by severe climate change

impacts. The hybrid ML-BGC modelling is thought as a tool that benefits from the interpretability of numerical simulations and the capabilities of ML models. In particular, numerical simulations enable to capture causal relationships behaviours. At the same time, ML, with its advanced extrapolation and generalization capabilities relying on data, might be able to detect additional phenomena that are not captured by the causal relationships (e.g., increasing variability and extreme values). Results showed that the developed ML model, trained, validated and tested on the observed data, produced satisfactory results, with good accuracy in predicting the Chl-a indicator (i.e., 0.61 median classification, 0.80 quartiles classification). This outcome confirms the ability of the RF algorithm to learn trends and patterns from historical data. Secondly, with regard to future Chl-a scenarios under climate change conditions, the hybrid ML-BGC model show a decreasing trend in lower Chl-a values for the far future (2100), while an increasing pattern for the higher ones. Finally, analysing seasonalises, summer remains the season with the highest Chl-a values in all scenarios, although in 2100 an increase in Chl-a values is also expected during the spring season as a consequence of the prospected anticipated optimal conditions for algal proliferation (e. g., a temperature around 25 °C, abundant light, and stable wind conditions), due to climate change.

Laying the groundwork for further analysis, the proposed hybrid framework shows proper flexibility to be applied in other case studies characterized by similar environmental features and issues, as well as data availability. It provides accessible modelling and scenario analysis services, and it is reusable and interoperable. Understanding how WQ responds to climate variations, and advancing in the digital knowledge

services may facilitate the pathway towards the identification of appropriate adaptation and mitigation measures against WQ degradation in the water bodies (e.g., wetlands restorations), paving the way for a transformative change in climate adaptation pathways, as recommended by the EU Mission Starfish 2030. The contribution of the presented methodology help in the advancing of the digital transformation in the field of WQ evaluation and prediction. Progress that can strength social actors and stakeholders who require standardized, easy-to-implement, and robust methods in support of meaningfully climate-proof measures for mid and far future water bodies good status.

CRediT authorship contribution statement

F. Zennaro: Conceptualization, Data curation, Formal analysis, Methodology, Investigation, Visualization, Writing – original draft. **E. Furlan:** Conceptualization, Methodology, Funding acquisition, Investigation, Writing – original draft. **D. Canu:** Conceptualization, Methodology, Investigation, Writing – original draft. **L. Aveytua Alcazar:** Data curation, Formal analysis, Methodology, Investigation, Writing – original draft. **G. Rosati:** Data curation, Formal analysis, Methodology, Investigation, Writing – original draft. **C. Solidoro:** Investigation, Validation, Writing – review & editing. **S. Aslan:** Data curation, Methodology. **A. Critto:** Funding acquisition, Supervision, Conceptualization, Validation, Writing – review & editing.

Declaration of Competing Interest

The authors declare that they have no known competing financial interests or personal relationships that could have appeared to influence the work reported in this paper.

Data availability

Data will be made available on request.

Acknowledgements

Appendix A. Supplementary data

Supplementary data to this article can be found online at https://doi.org/10.1016/j.ecolind.2023.111245.

References

Acri, F., Braga, F., Aubry, F.B., 2020. Long-term dynamics in nutrients, chlorophyll a and water quality parameters in the lagoon of venice. Sci. Mar. 84 (3), 215–225. https://doi.org/10.3989/scimar.05022.30A.

Ahmed, U., Mumtaz, R., Anwar, H., Shah, A.A., Irfan, R., García-Nieto, J., 2019. Efficient water quality prediction using supervised machine learning. Water 11 (11), 2210.

Al-Taee, I. A. A. (2018). Salinity effect chlorophyll significantly. Plant Archives, 18(1), 723–726. ISSN 0972-5210. https://www.plantarchives.org/PDF%20181/723-726%20(PA3%204182).pdf.

Anthony, A., Atwood, J., August, P., Byron, C., Cobb, S., Foster, C., Fry, C., Gold, A., Hagos, K., Heffner, L., Kellogg, D.Q., Lellis-Dibble, K., Opaluch, J.J., Oviatt, C., Pfeiffer-Herbert, A., Rohr, N., Smith, L., Smythe, T., Swift, J., Vinhateiro, N., 2009. Coastal lagoons and climate change: Ecological and social ramifications in U.S. Atlantic and Gulf coast ecosystems. Ecol. Soc. 14 (1) https://doi.org/10.5751/ES-02719-140108.

Aslan, S., Zennaro, F., Furlan, E., Critto, A., 2022. Recurrent neural networks for water quality assessment in complex coastal lagoon environments: A case study on the

Venice Lagoon. Environ. Model. Softw. 154 (May), 105403 https://doi.org/10.1016/j.envsoft.2022.105403.

Barzegar, R., Aalami, M.T., Adamowski, J., 2020. Short-term water quality variable prediction using a hybrid CNN–LSTM deep learning model. Stoch. Env. Res. Risk A. 34 (2), 415–433. https://doi.org/10.1007/s00477-020-01776-2.

Baxter, J. M. (2019). Ocean deoxygenation: everyone's problem. Causes, impacts, consequences and solutions. In Ocean deoxygenation: everyone's problem. Causes, impacts, consequences and solutions. https://doi.org/10.2305/iucn.ch.2019.13.en.

Bednar-Friedl, B., Biesbroek, R., Schmidt, D. N., Alexander, P., Børsheim, K. Y., Carnicer, J., Georgopoulou, E., Haasnoot, M., Cozannet, G. Le, Lionello, P., Lipka, O., Möllmann, C., Muccione, V., Mustonen, T., Piepenburg, D., & Whitmarsh, L. (2022). Europe. In: Climate Change 2022: Impacts, Adaptation and Vulnerability. Contribution. https://doi.org/10.1017/9781009325844.015.

Bendoricchio, G., De Boni, G., 2005. A water-quality model for the Lagoon of Venice. Italy. Ecological Modelling 184 (1), 69–81. https://doi.org/10.1016/j.ecolmodel.2004.11.013.

Bernardi Aubry, F., Acri, F., Finotto, S., Pugnetti, A., 2021. Phytoplankton dynamics and water quality in the venice lagoon. Water (switzerland) 13 (19). https://doi.org/10.3390/w13192780.

Borisova, J., Aladina, A., Nikitin, N.O., 2021. Hybrid modelling of environmental processes using composite models. Procedia Computer Science 193, 256–265.

Brazil, J.A.M., Alfaro, E., Rica, C., France, F.A., Uk, J.B., Becker, N., 2008. IPCC–Intergovernmental Panel on Climate Change. Choice Reviews. Online 45 (09). https://doi.org/10.5860/choice.45-5008.

Breitburg, D., Levin, L. A., Oschlies, A., Grégoire, M., Chavez, F. P., Conley, D. J., Garçon, V., Gilbert, D., Gutiérrez, D., Isensee, K., Jacinto, G. S., Limburg, K. E., Montes, I., Naqvi, S. W. A., Pitcher, G. C., Rabalais, N. Roman, N., Rose, M. R., Seibel, K. A., B. A., … Zhang, J. (2018). Declining oxygen in the global ocean and coastal waters. Science, 359(6371). https://doi.org/10.1126/science.aam7240.

Breiman, L., Ihaka, R., 1984. *Nonlinear discriminant analysis via scaling and ACE.* Davis One Shields Avenue, Davis, CA, USA.

Bucchignani, E., Montesarchio, M., Zollo, A.L., Mercogliano, P., 2016. High-resolution climate simulations with COSMO-CLM over Italy: performance evaluation and climate projections for the 21st century. Int. J. Climatol. 36 (2), 735–756.

Caretta, M. A., Mukherji, A., Arfanuzzaman, M., Betts, R. A., Gelfan, A., Hirabayashi, Y., Lissner, T. K., Liu, J., Gunn, E. L., Morgan, R., Mwanga, S., & Supratid, S. (2022). Water. In: Climate Change 2022: Impacts, Adaptation and Vulnerability (Vol. 15, Issue 2). https://doi.org/10.1017/9781009325844.006.552.

Canu, D.M., Solidoro, C., Cossarini, G., Giorgi, F., 2010. Effect of global change on bivalve rearing activity and the need for adaptive management. Climate Research 42 (1), 13–26.

Čehovin, L., Bosnić, Z., 2010. Empirical evaluation of feature selection methods in classification. Intell. Data Anal. 14 (3), 265–281. https://doi.org/10.3233/IDA-2010-0421.

Çevirgen, S., Elwany, H., Pesce, M., et al., 2020. Managing nutrient pollution in Venice Lagoon (Italy): a practical tool for assessment of water quality. Sustain. Water Resour. Manag. 6, 33. https://doi.org/10.1007/s40899-020-00390-y.

Chen, Y., Song, L., Liu, Y., Yang, L., Li, D., 2020. A review of the artificial neural network models for water quality prediction. Applied Sciences (switzerland) 10 (17). https://doi.org/10.3390/app10175776.

Chicco, D., Jurman, G., 2020. The advantages of the Matthews correlation coefficient (MCC) over F1 score and accuracy in binary classification evaluation. BMC Genomics 21 (1), 1–13. https://doi.org/10.1186/s12864-019-6413-7.

Ciavatta, S., Pastres, R., Badetti, C., Ferrari, G., Beck, M.B., 2008. Estimation of phytoplanktonic production and system respiration from data collected by a real-time monitoring network in the Lagoon of Venice. Ecol. Model. 212 (1–2), 28–36. https://doi.org/10.1016/j.ecolmodel.2007.10.025.

Cloern, J.E., 2001. Our evolving conceptual model of the coastal eutrophication problem. Mar. Ecol. Prog. Ser. 210, 223–253. https://doi.org/10.3354/MEPS210223.

Cossarini, G., Libralato, S., Salon, S., Gao, X., Giorgi, F., Solidoro, C., 2008. Downscaling experiment for the Venice lagoon. II. Effects of changes in precipitation on biogeochemical properties. Climate Res. 38 (1), 43–59. https://doi.org/10.3354/CR00758.

Cucco, A., Umgiesser, G., 2006. Modeling the Venice Lagoon residence time. Ecol. Model. 193 (1), 34–51.

de Backer, E., Aertsens, J., Vergucht, S., Steurbaut, W., 2009. Assessing the ecological soundness of organic and conventional agriculture by means of life cycle assessment (LCA). Br. Food J. 111 (10), 1028–1061. https://doi.org/10.1108/00070700910992916.

Derot, J., Yajima, H., Jacquet, S., 2020. Advances in forecasting harmful algal blooms using machine learning models: A case study with Planktothrix rubescens in Lake Geneva. Harmful Algae 99 (September), 101906. https://doi.org/10.1016/j.hal.2020.101906.

EC. (2000). Directive 2000/60/EC of the European Parliament and of the Council of 23 October 2000 establishing a framework for Community action in the field of water policy. Official Journal of the European Parliament. https://doi.org/10.1039/ap9842100196.

Facca, C., Bilaničovà, D., Pojana, G., Sfriso, A., Marcomini, A., 2014. Harmful algae records in venice lagoon and in Po River Delta (Northern Adriatic Sea, Italy). Scientific World Journal 2014. https://doi.org/10.1155/2014/806032.

Gačić, M., Mosquera, I.M., Kovačević, V., Mazzoldi, A., Cardin, V., Arena, F., Gelsi, G., 2004. Temporal variations of water flow between the Venetian lagoon and the open sea. Journal of Marine Systems 51 (1–4), 33–47.

García Nieto, P.J., García-Gonzalo, E., Alonso Fernández, J.R., Díaz Muñiz, C., 2019. Water eutrophication assessment relied on various machine learning techniques: A

case study in the Englishmen Lake (Northern Spain). Ecol. Model. 404 (February), 91–102. https://doi.org/10.1016/j.ecolmodel.2019.03.009.

Glibert, P.M., June 2019. Harmful algae at the complex nexus of eutrophication and climate change. Harmful Algae 91. https://doi.org/10.1016/j.hal.2019.03.001.

Grafton, R.Q., Williams, J., Perry, C.J., Molle, F., Ringler, C., Steduto, P., Allen, R.G., 2018. The paradox of irrigation efficiency. Science 361 (6404), 748–750.

Håkanson, L., Eklund, J., 2010. Relationships Between Chlorophyll, Salinity, Phosphorus, and Nitrogen in Lakes and Marine Areas. J. Coast. Res. 26, 412–423. https://doi.org/10.2112/08-1121.1.

Han, H., Guo, X., Yu, H., 2016. Variable selection using Mean Decrease Accuracy and Mean Decrease Gini based on Random Forest. In: 2016 7th IEEE International Conference on Software Engineering and Service Science (ICSESS), pp. 219–224. https://doi.org/10.1109/ICSESS.2016.7883053.

Hastie, T., Tibshirani, R., & Friedman, J. (2009). The Elements of Statistical Learning. SSS. Springer, New York. https://doi.org/10.1007/978-0-387-84858-7.

Intergovernmental Panel on Climate Change. (2014). Climate Change 2014: Synthesis Report. Contribution of Working Groups I, II and III to the Fifth Assessment Report of the Intergovernmental Panel on Climate Change (Core Writing TeamPachauri RK, Meyer LA (eds)). IPCC, Geneva, Switzerland. In Climate Change 2014 Mitigation of Climate Change. Cambridge University Press. https://doi.org/10.1017/CBO9781107415416.

Ishwaran, X. C. and H. (2012). Random Forests for Genomic Data Analysis. Genomics, 23 (1), 1–7. https://doi.org/10.1016/j.ygeno.2012.04.003.Random.

Jane, S.F., Hansen, G.J.A., Kraemer, B.M., Leavitt, P.R., Mincer, J.L., North, R.L., Pilla, R. M., Stetler, J.T., Williamson, C.E., Woolway, R.I., Arvola, L., Chandra, S., DeGasperi, C.L., Diemer, L., Dunalska, J., Erina, O., Flaim, G., Grossart, H.P., Hambright, K.D., Rose, K.C., 2021. Widespread deoxygenation of temperate lakes. Nature 594 (7861), 66–70. https://doi.org/10.1038/s41586-021-03550-y.

Kotsiantis, S.B., Zaharakis, I.D., Pintelas, P.E., 2006. Machine learning: A review of classification and combining techniques. Artif. Intell. Rev. 26 (3), 159–190. https://doi.org/10.1007/s10462-007-9052-3.

Kwiatkowski, L., Torres, O., Bopp, L., Aumont, O., Chamberlain, M., Christian, J.R., Dunne, J.P., Gehlen, M., Ilyina, T., John, J.G., Lenton, A., Li, H., Lovenduski, N.S., Orr, J.C., Palmieri, J., Santana-Falcón, Y., Schwinger, J., Séférian, R., Stock, C.A., Ziehn, T., 2020. Twenty-first century ocean warming, acidification, deoxygenation, and upper-ocean nutrient and primary production decline from CMIP6 model projections. Biogeosciences 17 (13), 3439–3470. https://doi.org/10.5194/bg-17-3439-2020.

L'Heureux, A., Grolinger, K., Elyamany, H.F., Capretz, M.A.M., 2017. Machine Learning with Big Data: Challenges and Approaches. IEEE Access 5 (April), 7776–7797. https://doi.org/10.1109/ACCESS.2017.2696365.

Lloret, J., Marín, A., Marín-Guirao, L., 2008. Is coastal lagoon eutrophication likely to be aggravated by global climate change? Estuar. Coast. Shelf Sci. 78 (2), 403–412. https://doi.org/10.1016/j.ecss.2008.01.003.

Mack, L., Andersen, H.E., Beklioğlu, M., Bucak, T., Couture, R.M., Cremona, F., Ferreira, M.T., Hutchins, M.G., Mischke, U., Molina-Navarro, E., Rankinen, K., Venohr, M., Birk, S., 2019. The future depends on what we do today – Projecting Europe's surface water quality into three different future scenarios. Sci. Total Environ. 668 (February), 470–484. https://doi.org/10.1016/j.scitotenv.2019.02.251.

Maier, P.M., Keller, S., 2019. ESTIMATING CHLOROPHYLL A CONCENTRATIONS OF SEVERAL INLAND WATERS WITH HYPERSPECTRAL DATA AND MACHINE LEARNING MODELS, ISPRS Ann. Photogramm. Remote Sens. Spatial Inf. Sci. IV-2/W5, 609–614. https://doi.org/10.5194/isprs-annals-IV-2-W5-609-2019.

Maindonald, J.H., 2013. Data Analysis and Data Mining: An Introduction by Adelchi Azzalini, Bruno Scarpa. Int. Stat. Rev. 81, 170–171. https://doi.org/10.1111/insr.12011_23.

Marzban, C., 2009. Basic statistics and basic AI: Neural networks. Artificial Intelligence Methods in the Environmental Sciences 15–47. https://doi.org/10.1007/978-1-4020-9119-3_2.

MAV. (2008). Ufficio di Piano Attività di salvaguardia di Venezia e della sua laguna: lo stato ecologico della laguna Rapporto Tematico.

Melaku Canu, D., Aveytua, L., Laurent, C., Lazzari, P., Rosati, G., Solidoro, C., 2023. The Lagoon of Venice Climate scenarios projections with the finite element hydrodynamic model SHYFEM-BFM. ISEM 2023. The International Society of Ecological Modelling Global Conference.

Melesse, A.M., Krishnaswamy, J., Zhang, K., 2008. Modeling Coastal Eutrophication at Florida Bay using Neural Networks. J. Coast. Res. 2, 190–196. https://doi.org/10.2112/06-0646.1.

Miall, C., 1992. Understanding Neural Networks. Trends Neurosci. 15 (11), 464–465. https://doi.org/10.1016/0166-2236(92)90012-w.

Morucci, S., Coraci, E., Crosato, F., Ferla, M., 2020. Extreme events in Venice and in the North Adriatic Sea: 28–29 October 2018. Rendiconti Lincei 31 (1), 113–122. https://doi.org/10.1007/s12210-020-00882-1.

Myers, L., Sirois, M.J., 2006. Spearman Correlation Coefficients. Differences between, In Encyclopedia of Statistical Sciences https://doi.org/https://doi.org/10.1002/0471667196.ess5050.pub2.

Nazeer, M., Id, M.B., Alsahli, M.M.M., Shahzad, M.I., Waqas, A., 2017. Evaluation of Empirical and Machine Learning Algorithms for Estimation of Coastal Water Quality Parameters. https://doi.org/10.3390/ijgi6110360.

Nelson, N.G., Munoz-Carpena, R., Phlips, E.J., Kaplan, D., Sucsy, P., Hendrickson, J., 2018. Revealing Biotic and Abiotic Controls of Harmful Algal Blooms in a Shallow Subtropical Lake through Statistical Machine Learning. Environ. Sci. Tech. 52 (6), 3527–3535. https://doi.org/10.1021/acs.est.7b05884.

Newton, A., Brito, A.C., Icely, J.D., Delorez, V., Clara, I., Angus, S., Schernewski, G., Inacio, M., Lillebø, A.I., Sousa, A.I., Ɓejaoui, B., Solidoro, C., Tosic, M., Canedo-

Argüelles, M., Yamamuro, M., Reizopoulou, S., Tseng, H., Canu, D., Roselli, L., Maanan, M., Cristina, S., Ruiz-Fernandez, A.C., Lima, R., Kjerfve, B., RubioCisneros, N., Ṕerez-Ruzafa, A., Marcos, C., Pastres, R., Pranovi, F., Snoussi, M., Turpie, J., Tuchkovenko, Y., Dyack, B., Brookes, J., Povilankas, R., Khokhlov, V., 2018. Assessing, quantifying and valuing the ecosystem services of coastal lagoons. J. Nat. Conserv. 44, 50–65. https://doi.org/10.1016/j.jnc.2018.02.009.

Politikos, D.V., Petasis, G., Katselis, G., 2021. Interpretable machine learning to forecast hypoxia in a lagoon. Eco. Inform. 66 (July), 101480 https://doi.org/10.1016/j.ecoinf.2021.101480.

Reale, M., Cossarini, G., Lazzari, P., Lovato, T., Bolzon, G., Masina, S., et al., 2022. Acidification, deoxygenation, nutrient and biomasses decline in a warming Mediterranean Sea. Biogeosciences Discuss. https://doi.org/10.5194/bg-2021-301.

Riahi, K., Rao, S., Krey, V., Cho, C., Chirkov, V., Fischer, G., Kindermann, G., Nakicenovic, N., Rafaj, P., 2011. RCP 8.5-A scenario of comparatively high greenhouse gas emissions. Clim. Change 109 (1), 33–57. https://doi.org/10.1007/s10584-011-0149-y.

Runca, E., Bernstein, A., Postma, L., & Di Silvio, G. (1996). Control of macroalgae blooms in the Lagoon of Venice. Ocean and Coastal Management, 30(2–3), 235–257. https://doi.org/10.1016/0964-5691(95)00065-8.

Runca, E., Bernstein, A., Postma, L., Di Silvio, G., 1996. Control of macroalgae blooms in the Lagoon of Venice. Ocean & coastal management 30 (2–3), 235–257.

Salon, S., Cossarini, G., Libralato, S., Gao, X., Solidoro, C., Giorgi, F., 2008. Downscaling experiment for the Venice lagoon. I. Validation of the present-day precipitation climatology. Climate Res. 38 (1), 31–41. https://doi.org/10.3354/CR00758.

Warren S. Sarle. (1994). Neural Networks and Statistical Models Proceedings of the Nineteenth Annual SAS Users Group International Conference. https://api.semanticscholar.org/CorpusID:2562349.

Sfriso, A., Facca, C., Ghetti, P.F., 2009. Validation of the Macrophyte Quality Index (MaQI) set up to assess the ecological status of Italian marine transitional environments. Hydrobiologia 617, 117–141.

Sfriso, A., Pavoni, B., Marcomini, A., 1989. Macroalgae and phytoplankton standing crops in the central Venice lagoon: Primary production and nutrient balance. Science of the Total Environment, the 80 (2–3), 139–159. https://doi.org/10.1016/0048-9697(89)90070-3.

Sfriso, A., Pavoni, B., Marcomini, A., Orio, A.A., 1992. Macroalgae, nutrient cycles, and pollutants in the Lagoon of Venice. Estuaries 15 (4), 517–528. https://doi.org/10.2307/1352394.

Sen Gupta, A., Thomsen, M., Benthuysen, J.A., Hobday, A.J., Oliver, E., Alexander, L.V., Smale, D.A., 2020. Drivers and impacts of the most extreme marine heatwave events. Scientific reports 10 (1), 19359.

Sfriso, A., Buosi, A., Mistri, M., Munari, C., Franzoi, P., Sfriso, A.A., 2019. Long-term changes of the trophic status in transitional ecosystems of the northern Adriatic Sea, key parameters and future expectations: The lagoon of Venice as a study case. Nature Conservation 34, 193–215. https://doi.org/10.3897/natureconservation.34.30473.

Shalby, A., Elshemy, M., Zeidan, B.A., 2020. Assessment of climate change impacts on water quality parameters of Lake Burullus. Egypt. Environmental Science and Pollution Research 27 (26), 32157–32178. https://doi.org/10.1007/s11356-019-06105-x.

Solidoro, C., Pastres, R., Cossarini, G., Ciavatta, S., 2004. Seasonal and spatial variability of water quality parameters in the lagoon of Venice. J. Mar. Syst. 51 (1–4 SPEC. ISS.), 7–18. https://doi.org/10.1016/j.jmarsys.2004.05.024.

Solidoro, C., Cossarini, G., Lazzari, P., Galli, G., Bolzon, G., Somot, S., et al., 2022. Modeling carbon budgets and acidification in the Mediterranean Sea ecosystem under contemporary and future climate. Front. Mar. Sci. 8 https://doi.org/10.3389/fmars.2021.781522.

Solidoro, C., Cossarini, G., Libralato, S., Salon, S., 2010. Remarks on the redefinition of system boundaries and model parameterization for downscaling experiments. Prog. Oceanogr. 84 (1–2), 134–137.

Teruzzi, A., Di Cerbo, P., Cossarini, G., Pascolo, E., Salon, S., 2019. Parallel implementation of a data assimilation scheme for operational oceanography: The case of the MedBFM model system. Comput. Geosci. 124, 103–114. https://doi.org/10.1016/j.cageo.2019.01.003.

Tong, Y., Xu, X., Zhang, S., Shi, L., Zhang, X., Wang, M., 2019. Establishment of Season-Speci Fi c Nutrient Thresholds and Analyses of the e Ff Ects of Nutrient Management in Eutrophic Lakes through Statistical Machine Learning. 578 (August) https://doi.org/10.1016/j.jhydrol.2019.124079.

Uusitalo, L., Blenckner, T., Puntila-Dodd, R., Skyttä, A., Jernberg, S., Voss, R., Müller-Karulis, B., Tomczak, M.T., Möllmann, C., Peltonen, H., 2022. Integrating diverse model results into decision support for good environmental status and blue growth. Sci. Total Environ. 806, 150450 https://doi.org/10.1016/J.SCITOTENV.2021.150450.

Veneto, A.R.P.A., 2013. Moria di pesci nella Laguna di Venezia. Il Meteo Della Primavera Ha Favorito Il Proliferare Delle Alghe. https://www.arpa.veneto.it/arpavinform a/comunicati-stampa/archivio/comunicati-2013/moria-di-pesci-nella-laguna-di-ven ezia.-il-meteo-della-primavera-ha-favorito-il-proliferare-delle-alghe/?searchterm=al ghe.

ARPA Veneto. (2021). Rete stato ambientale. 3–5. https://www.arpa.veneto.it/temi-ambientali/acqua/acque-di-transizione/laguna-di-venezia/la-rete-di-monitoraggio/rete-stato-ambientale.

Vinçon-Leite, B., Casenave, C., 2019. Modelling eutrophication in lake ecosystems: A review. Sci. Total Environ. 651, 2985–3001. https://doi.org/10.1016/j.scitotenv.2018.09.320.

Zanchettin, D., Bruni, S., Raicich, F., Lionello, P., Adloff, F., Androsov, A., Antonioli, F., Artale, V., Carminati, E., Ferrarin, C., Fofonova, V., Nicholls, R.J., Rubinetti, S., Rubino, A., Sannino, G., Spada, G., Thiéblemont, R., Tsimplis, M., Umgiesser, G., Zerbini, S., 2021. Sea-level rise in Venice: Historic and future trends (review article).

Nat. Hazards Earth Syst. Sci. 21 (8), 2643–2678. https://doi.org/10.5194/nhess-21-2643-2021.

Zennaro, F., Furlan, E., Simeoni, C., Torresan, S., Aslan, S., Critto, A., Marcomini, A., 2021. Exploring machine learning potential for climate change risk assessment. Earth Sci. Rev. 220 (February), 103752 https://doi.org/10.1016/j.earscirev.2021.103752.

Zuliani, A., Zaggia, L., Collavini, F., Zonta, R., 2005. Freshwater discharge from the drainage basin to the Venice Lagoon (Italy). Environ. Int. 31 (7 SPEC. ISS.), 929–938. https://doi.org/10.1016/j.envint.2005.05.004.

Umgiesser, G., Melaku Canu, D., Cucco, A., Solidoro, C. 2004. A finite element model for the Venice Lagoon. Development, set up, calibration and validation Journal of Marine Systems, Volume 51, Issues 1-4, pp. 123-145.

Vichi, M., Lovato, T., Butenschön, M., Tedesco, L., Lazzari, P., Cossarini, G., Masina, S., Pinardi, N., Solidoro, C., Zavatarelli, M. (2020). The Biogeochemical Flux Model (BFM): Equation Description and User Manual. BFM version 5.2. BFM Report series N. 1, Release 1.2, June 2020, Bologna, Italy, http://bfm-community.eu, pp. 104.